



Contents lists available at ScienceDirect



# Catalysis Today

journal homepage: [www.elsevier.com/locate/cattod](http://www.elsevier.com/locate/cattod)

## Quantitative infrared spectroscopic studies and 2D COS analysis of xylenes isomerization over hierarchical zeolites

Karolina A. Tarach <sup>a,\*</sup>, Kinga Gołabek <sup>a</sup>, Minkee Choi <sup>b</sup>, Kinga Góra-Marek <sup>a</sup>

<sup>a</sup> Faculty of Chemistry, Jagiellonian University in Kraków, 3 Ingardena St., 30-060 Kraków, Poland

<sup>b</sup> Department of Chemical and Biomolecular Engineering, Korea Advanced Institute of Science and Technology, Daejeon 305-701, Republic of Korea

### ARTICLE INFO

#### Article history:

Received 31 October 2015

Received in revised form 14 January 2016

Accepted 18 February 2016

Available online xxx

#### Keywords:

2D COS analysis

Xylene

Isomerization

Hierarchical zeolites

ZSM-5

### ABSTRACT

The microporous and hierarchical ZSM-5 zeolites were studied with respect to their interaction with *o*-, *m*- and *p*-xylene molecules as well as the catalytic activity in xylenes isomerization process followed by 2D COS analysis of IR spectra. The aspects of mechanism of xylene isomerization reaction have been discussed in the light of the results of 2D COS analysis of IR spectra and catalytic performance of studied zeolites. The ZSM-5 zeolites were characterized by different Si/Al ratio and by various types of generated mesoporosity. This selection assured ability to follow properly the changes in the catalytic performance related not only to acidic properties but also to porosity of the samples. It was shown that the microporous character of zeolites was crucial for high selectivity to the most desired product i.e. *p*-xylene. In the case of hierarchical zeolites it was confirmed that the formation of by-products as mesitylene and toluene occurred during ortho-xylene isomerization. Furthermore, for hierarchical zeolites the high amount of silanols groups prompted to the coke formation on highly developed external surface.

© 2016 Elsevier B.V. All rights reserved.

### 1. Introduction

The ZSM-5 zeolite is widely applied in several industrial processes requiring the shape-selectivity, including alkylation, isomerization and disproportionation [1–3]. During xylene transformation process two main reactions can take place: (i) isomerization, which is aimed to increase the relative content of *p*-xylene and (ii) disproportionation leading to trimethylbenzene and toluene in equal amounts. It well know that the isomerization reaction occurs through the monomolecular mechanism while the disproportionation involves the bimolecular mechanism with bulky intermediates [4].

The 2D COS analysis of spectroscopy results was developed by Noda [5] and initially applied to the studies of sinusoidal changes in IR absorbance spectra of polymer upon mechanical strain. Further development of 2D COS analysis allowed operating with systems changed upon non-periodical variables as in the case of chemical processes undergoing on surface of catalyst. The 2D COS analysis is based on Fourier transform, which is used to extract spectral correlations occurring upon external modulation of system. As a result a 3D graph of changes in spectra is obtained with two axes for

wavenumbers and one for correlation level, expressed as intensity. In synchronous correlation applied in this study the observed on diagonal positive auto-peaks represent each varying band at given wavenumber. The positive correlation between two separate bands (of different wavenumbers) represents the simultaneous increase or decrease in intensity of these bands. On the other hand, the negative correlation occurs when one of the bands changes its intensity at the expense of the other one. The use of 2D COS analysis significantly enhanced the use of IR spectroscopy to following even the slightest changes in IR spectrum during heterogeneous reactions at high temperatures [6].

The synthesis of hierarchically structured zeolites are performed according to two different approaches. *Bottom-up* approaches provide the control during synthesis and employ either various types of templates (e.g. surfactants, porous carbon, cationic polymers, etc.) [7–10] or concern zeolitization of mesoporous materials [11]. Also direct synthesis of nanosized crystals [12,13] is in the field of interest of researchers. Hierarchical zeolites obtained in the presence of surfactants contain the acid sites of high concentration and strength, and the additional uniform mesoporosity improves the accessibility of acid sites to reactants. The tuning of both the shape and the size of pores is a matter of template strategy. On the other hand, a selective extraction of silica (via desilication) [14–16] or alumina (via dealumination) [17] is the most common of *top-down* strategies. The demetalation processes led to the formation of zeo-

\* Corresponding author.

E-mail address: [karolina.tarach@gmail.com](mailto:katarzyna.tarach@gmail.com) (K.A. Tarach).

lites with bimodal porosity and are known as the most effective approaches for obtaining the hierarchical zeolites. The steaming of zeolite Y and desilication of ZSM-5 zeolite are well-known examples [18–20]. The number of framework silicon or aluminium atoms that could be removed without structural damage is ruled by the features inherent to zeolites (Si/Al ratio and framework topology) as well as by the alkaline treatment conditions (type and concentration of agents used). Both processes not only create mesopores, but also affect the acidity of hierarchical zeolite mainly by modifying the nature of acidic sites [14,21].

The studies concerning the use of 2D COS analysis of IR spectra to follow the heterogeneous reaction of xylene isomerization are quite limited. The results presented by several authors have concerned the *o*-xylene isomerization process over H-ZSM-5 zeolites. The role of porosity and acidity during isomerization has been mostly studied in context of coke deposition [6,22,23]. This work was attempted to offer an insight into acidity and porosity properties of microporous and hierarchical ZSM-5 zeolites in respect to their interaction with xylene molecules and also their catalytic performance in xylene isomerization process. The range of materials studied in this paper, typically microporous ZSM-5 and their hierarchical analogues obtained by different methods, however representing at some points similar properties, allowed following the influence of acidity and porosity on xylene isomerization process. The application of 2D COS analysis to the results of time-resolved in-situ IR spectroscopy enabled following even the slightest changes in the spectra of reagents adsorbed over studied zeolites. The correlation either positive or negative between diagnostic bands of xylene isomers provided valuable information on processes taking place during catalytic reaction. Both acidity and porosity of studied zeolites were significantly different depending on synthesis or modification procedure however they found the reflection in catalytic reactions.

## 2. Material and methods

### 2.1. Studied materials

Parent microporous ZSM-5 zeolite denoted as **B-ZSM-5** of Si/Al=32 was supplied by Zeolyst (CBV 5524G). The sample denoted as **D-ZSM-5** was obtained by desilication in the 0.2 M solution of NaOH&TBAOH (tetrabutylammonium hydroxide) mixture TBAOH/(NaOH + TBAOH)=0.1 at the temperature of 80 °C for 5 h. The 100 ml of solution was added to 3.0 g of zeolite. After desilication the suspension was cooled down in ice-bath, filtered and washed until neutral pH. Finally, the zeolites were again filtered, washed with distillate water, dried overnight at room temperature and calcined at 550 °C.

Carbon-black templated zeolite (denoted as **C-ZSM-5**) was synthesized using the gel composition of 2.0 NaCl: 1.67 Al<sub>2</sub>O<sub>3</sub>: 100 SiO<sub>2</sub>: 20 TPA<sub>2</sub>O: 200H<sub>2</sub>O. The added carbon-black was 100 wt% of the added silica. In a typical synthesis, 0.69 g NaCl and 4.0 g aluminium isopropoxide were dissolved in 212 g TPAOH (tetrapropylammonium hydroxide) solution (TCI, 20–25% in H<sub>2</sub>O). 122 g TEOS was added under vigorous stirring and the reaction mixture was stirred for 3 h at room temperature. Then, 35.2 g carbon black (HIBLACK 900 L, Evonik, average particle size: 15 nm, surface area: 270 m<sup>2</sup> g<sup>-1</sup>) was added and the mixture was stirred for 1 h for homogenization. The resultant mixture was heated at 90 °C on a hot plate under stirring to evaporate ethanol and extra H<sub>2</sub>O to obtain the aforementioned gel composition. The resultant synthesis gel was transferred into a Teflon-lined stainless-steel autoclave and hydrothermally crystallized at 180 °C for 72 h. After cooling to room temperature, the zeolite product was filtered and washed thoroughly with deionized water. The product was dried in an oven at 130 °C and subsequently calcined in air at 600 °C for 6 h.

Zeolite **M-ZSM-5** was obtained via a direct synthesis route using the amphiphilic organosilanes as a mesopore-directing agent [9]. For the synthesis of mesoporous zeolite M-ZSM-5 of Si/Al=29, the TPOAC (3-(trimethoxysilyl) propyl) octadecyldimethylammonium chloride (Aldrich, 42 wt% in methanol) was added to a conventional ZSM-5synthesis gel containing TPABr (tetrapropylammonium bromide). The molar synthesis composition was 43 Na<sub>2</sub>O: 5 Al<sub>2</sub>O<sub>3</sub>: 200 SiO<sub>2</sub>: 20 TPABr: 10 TPOAC: 15 H<sub>2</sub>SO<sub>4</sub>: 18000 H<sub>2</sub>O. In a typical synthesis, 1.77 g NaOH, 2.75 g TPABr, 6.09 g TPOAC, and 130 g H<sub>2</sub>O were dissolved in a polypropylene bottle. Then, 21.5 g TEOS (tetraethylorthosilicate) was added into the solution and stirred for 1 h. Then, 1.72 g Al<sub>2</sub>(SO<sub>4</sub>)<sub>3</sub> · 18H<sub>2</sub>O dissolved in 37.0 g H<sub>2</sub>O was added to the aforementioned solution and then homogenized by handshaking. The synthesis gel was stirred at room temperature for 24 h for aging. The resultant gel was hydrothermally treated in a tumbling autoclave at 170 °C for 72 h. After the hydrothermal crystallization, the precipitated products were filtered, washed with distilled water, dried at 110 °C and calcined at 550 °C [9].

### 2.2. Characterisation techniques

#### 2.2.1. X-ray diffraction (XRD)

Wide-angle XRD patterns were taken with a Rigaku Multiflex diffractometer equipped with Cu K $\alpha$  radiation (40 kV, 40 mA).

#### 2.2.2. Nitrogen sorption measurements at -196 °C

The nitrogen sorption measurements were performed on a Quantachrome Autosorb-1-MP gas sorption system at -196 °C. Prior to the measurements, all samples were degassed under high vacuum conditions for duration of 16 h at 200 °C. The micropore volume was calculated based on the t-plot method, while the Brunauer–Emmet–Teller (BET) method was applied to determine the apparent specific surface area, taking into account the recommendations of Rouquerol et al. [24]. Distributions of mesopore diameters were calculated via the Barrett–Joyner–Halenda (BJH) algorithm using the adsorption branch [25].

#### 2.2.3. STEM investigations

The STEM micrographs were obtained using transmission electron microscope (JEOL 2100F) working at 200 kV, with Field Emission Gun (FEG), EDX analysis and STEM detectors for bright and dark mode.

#### 2.2.4. IR spectroscopic studies

Prior to FTIR studies, the materials were pressed into the form of self-supporting discs (ca. 5–10 mg/cm<sup>2</sup>) and pre-treated in situ in an IR cell at 500 °C under vacuum conditions for 1 h. Time resolved FT-IR spectra were recorded with a Bruker Vertex 70 spectrometer equipped with a MCT detector. The spectral resolution was of 2 cm<sup>-1</sup>. All the spectra presented in this work were normalized to 10 mg of sample. The 2D-COS graphs were prepared with use of OPUS 3D software from Bruker Optics.

Total concentration of the Brønsted and Lewis acid sites in calibration materials was determined in quantitative IR studies of pyridine (hereafter denoted as Py) sorption according to the procedure described in Refs. [21,26]. Pyridine was supplied by Sigma-Aldrich ( $\geq$ 99.8%).

The concentrations of the Brønsted acid sites accessible for bulky pivalonitrile (hereafter denoted as Pn) was achieved from quantitative studies previously described in Refs. [27,28]. The pivalonitrile (98%, Sigma Aldrich) was adsorbed on the zeolites at room temperature followed by 20 min evacuation at the same temperature in order to remove the physisorbed probe. The concentration of the Brønsted and Lewis acid sites detected by Pn was calculated from the maximum intensities (the maximum heights) of the respective

bands at  $2277\text{ cm}^{-1}$  and  $2305\text{ cm}^{-1}$  and their extinction coefficients (0.11 and  $0.15\text{ cm}^2\text{ }\mu\text{mol}^{-1}$ , resp.).

### 3. Results and discussion

#### 3.1. Structural and textural characterization

The samples chosen for study were characterized by Si/Al ratio in range between 22 and 32, as well as by different level and type of developed mesoporosity (Table 1). This selection assured the ability to properly follow the changes in catalytic performance related not only to acidity but also to porosity of the samples (Table 1). The XRD patterns of the bulk B-ZSM-5 and carbon templated C-ZSM-5 zeolites demonstrated well resolved reflections representative for ZSM-5 structure (Fig. 1). Similar observation was made for hierarchical zeolite D-ZSM-5 obtained via top-down approach, i.e. desilication. Thus it can be concluded that the alkaline treatment did not perturb the crystallinity of resulting D-ZSM-5 material. The XRD pattern also confirmed formation of the ZSM-5 structure in the case of M-ZSM-5 zeolite synthesized by bottom-up route; however its lowered crystallinity can be considered in the terms of both highly developed mesoporosity and small size of zeolite grains. The synthesis process of M-ZSM-5 zeolite led to the generation of regularly distributed mesopores and enhanced surface area (Table 1 Fig. 2), thus high contribution of disordered surface.

The textural characteristics of studied hierarchical zeolites were derived from the low-temperature nitrogen sorption studies. Both B-ZSM-5 and C-ZSM-5 zeolites demonstrated the type-I  $\text{N}_2$  adsorption isotherm (Fig. 2a). The value of  $V_{\text{micro}} = 0.17\text{ cm}^3\text{ g}^{-1}$  point to the presence of microporosity typical of the MFI structure. Minor mesoporosity in both samples results from the interparticle space between the zeolite grains (Table 1). Indeed, the STEM images of

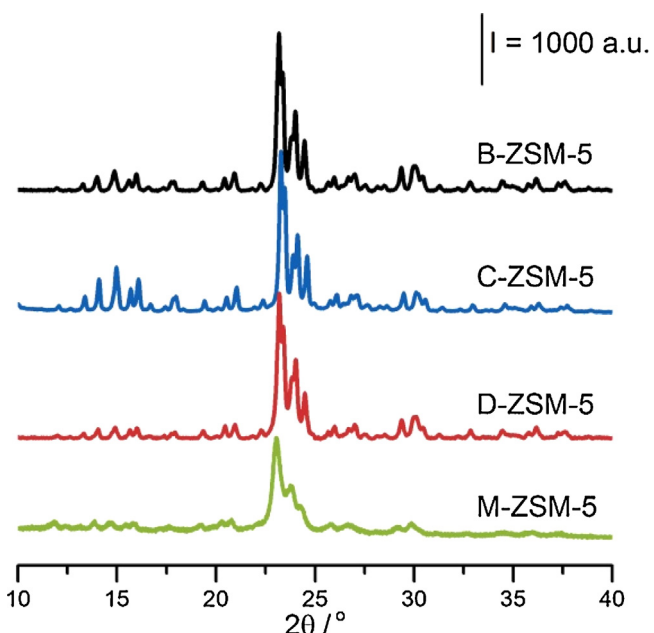


Fig. 1. XRD patterns of studied materials.

C-ZSM-5 zeolite showed that the synthesis procedure did not succeed in fabricating substantial mesoporosity, only the interparticle macroporosity is present (Fig. 3). The enhanced surface area  $S_{\text{BET}}$  and high contribution of micropore surface area point to the well-developed microporosity. This important characteristic of C-ZSM-5 should be underlined. The STEM images of B-ZSM-5 and C-ZSM-5

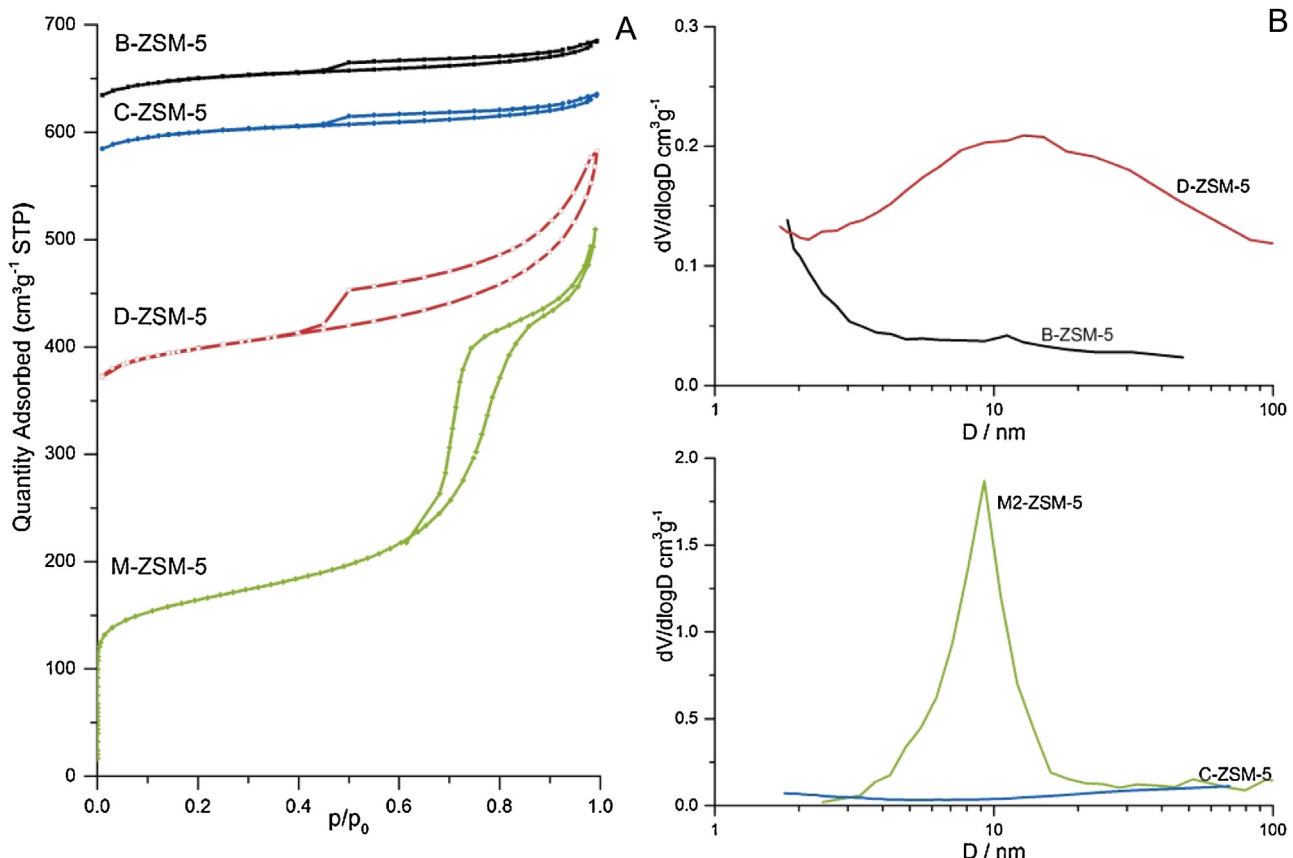
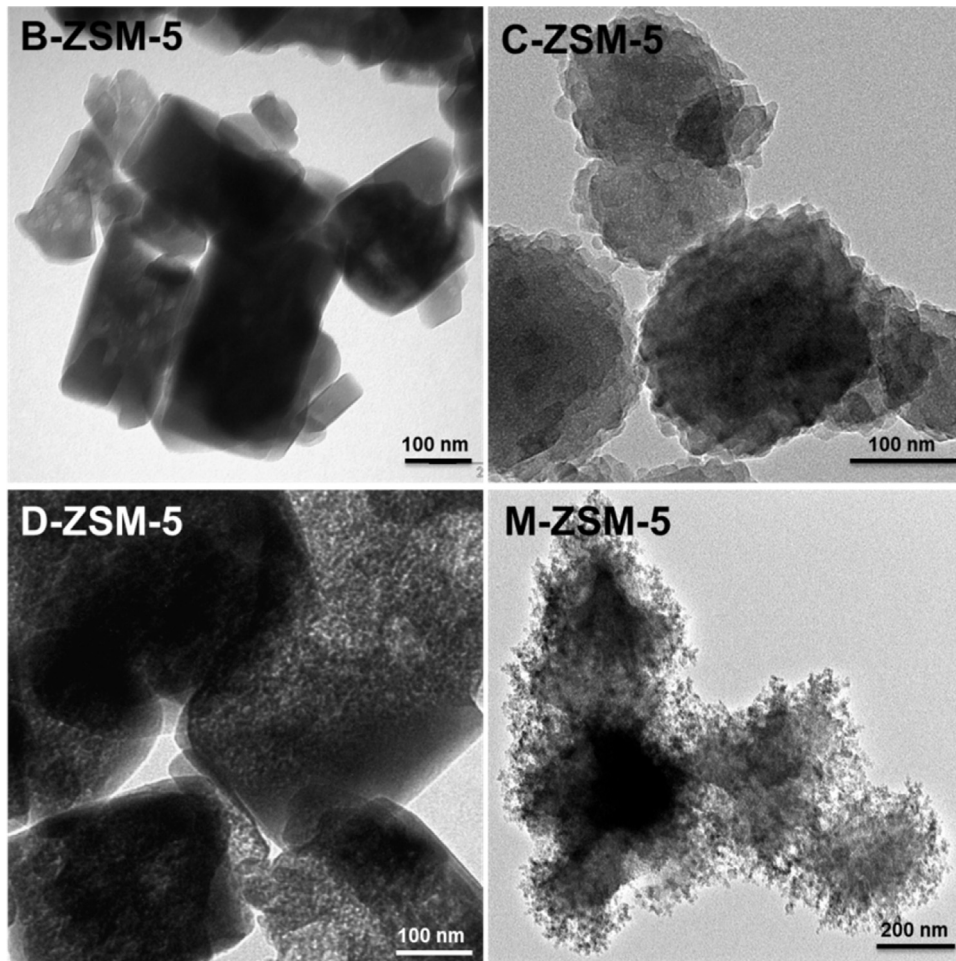


Fig. 2. (a) Low temperature  $\text{N}_2$  isotherms and (b) BJH pore size distributions of studied materials.

**Table 1**

The Si/Al ratios and the Al concentrations determined by chemical analysis ( $\text{Al}_{\text{ICP}}$ ), as well as the textural parameters from low temperature  $\text{N}_2$  adsorption/desorption measurements for studied zeolites.

Material	Si/Al	$\text{Al}_{\text{ICP}}$		$S_{\text{BET}}$ [ $\text{m}^2 \text{ g}^{-1}$ ]	$S_{\text{meso}}$ [ $\text{m}^2 \text{ g}^{-1}$ ]	$V_{\text{micro}}$ [ $\text{cm}^3 \text{ g}^{-1}$ ]	$V_{\text{meso}}$ [ $\text{cm}^3 \text{ g}^{-1}$ ]
		[-/u.c.]	[ $\mu\text{mol g}^{-1}$ ]				
B-ZSM-5	32	2.95	478	377	40	0.17	0.06
C-ZSM-5	30	3.10	502	459	44	0.17	0.08
D-ZSM-5	22	4.19	680	342	150	0.09	0.30
M-ZSM-5	29	3.20	518	520	187	0.16	0.35



**Fig. 3.** The STEM images of bulk and micro/mesoporous zeolites.

additionally provide information on various sizes of their grains, for B-ZSM-5 the grains size is in range of 150–300 nm while for C-ZSM-5 grains are formed from aggregates of a smaller size. The significant difference between the C-ZSM-5 and B-ZSM-5 samples is also seen in the shape of the zeolite crystal grains. The C-ZSM-5 sample is characterized by spherical grains with high surface roughness, on the other hand the B-ZSM-5 sample possess grains of bigger size and more rectangular shape. The top-down modified hierarchical zeolite D-ZSM-5 demonstrated a type-IV  $\text{N}_2$ -isotherm and showed the significant mesoporosity development upon alkaline treatment with preservation of the crystallinity. Upon alkaline treatment the development of mesopore surface area occurred at the expense of micropore area, thus the drop of  $V_{\text{micro}}$  was observed. Furthermore, in D-ZSM-5 zeolite the plugging of the micropores by extra-framework aluminium material is also expected, in line with IR acidity studies presented in Section 3.2.2. The STEM micrographs (Fig. 3) confirmed the formation of secondary mesoporosity directly inside the zeolite grains. Truly micro/mesoporous zeolite M-ZSM-5

also showed a type-IV  $\text{N}_2$ -isotherm with hysteresis loop at intermediate pressures, corresponding to the mesopores with maximum diameter at 9.2 nm (Fig. 2b). It is worth noticing that despite similar values of mesopore surface area the D-ZSM-5 and M-ZSM-5 samples significantly differ in the PSDs curves both in the maximum value reached and the pore diameters broadening. The STEM image of M-ZSM-5 zeolites (Fig. 3) indicated highly porous structure with small grains aggregated in globular structure.

The selection of the studied materials, from microporous ZSM-5 to micro/mesoporous analogues obtained by top-down and bottom-up methods, allows following the influence of porosity character and acidity on xylene isomerization process.

### 3.2. IR acidity characterization

#### 3.2.1. Analysis of the hydroxyls bands

Several well resolved bands of hydroxyl groups can be distinguished in the IR spectra of microporous and hierarchical zeolites

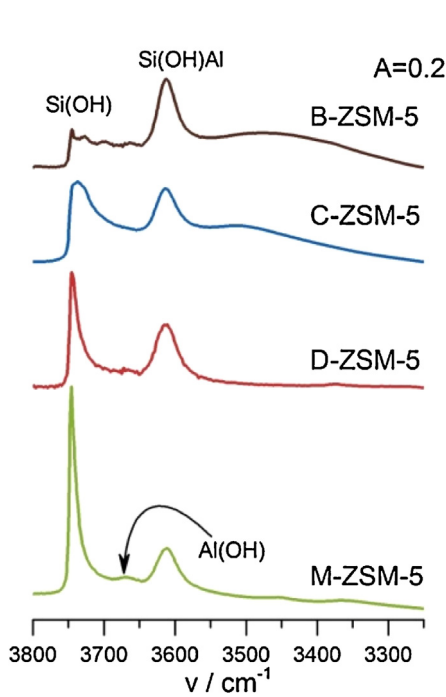


**Fig. 4.** IR spectra of studied materials in the region of O—H vibration.

(Fig. 4). The highest frequency band ( $3745\text{ cm}^{-1}$ ) represents the isolated silanols groups located on mesopore surface and on external surface of crystallites. Indeed, the intensity of isolated silanols band is significantly raised up for the hierarchical D-ZSM-5 and M-ZSM-5 zeolites. The  $3725\text{ cm}^{-1}$  band attributed to the vicinal silanols was found only in the spectra of B-ZSM-5 and C-ZSM-5 zeolites. Additionally, the presence of  $3690\text{ cm}^{-1}$  Al(OH) band of extra-framework non-acidic Al-species was detected in bulk zeolite B-ZSM-5. The acidic Si(OH)Al groups are represented by  $3610\text{ cm}^{-1}$  band. Both the intensities and the positions of these bands indicated the differentiated acidity of materials studied with regard to both the amount of sites and their strength.

### 3.2.2. Concentration and strength of acid sites

The concentrations of Brønsted and Lewis acid sites were calculated using the maximum heights of the  $1545\text{ cm}^{-1}$  band of pyridinium ions ( $\text{PyH}^+$ ) and of the  $1455\text{ cm}^{-1}$  band of coordinatively bonded pyridine to Lewis sites ( $\text{PyL}$ ), by applying the extinction coefficients equal  $0.07\text{ cm}^2/\mu\text{mol}$  and  $0.1\text{ cm}^2/\mu\text{mol}$ , respectively [21,26]. The quantitative studies of Py sorption indicated that the sum of Brønsted and Lewis acid sites concentrations is comparable with the total Al concentration from chemical analysis for all studied samples (Table 2). Purely microporous zeolites contained comparable amount of Brønsted acid sites; the C-ZSM-5 additionally maintained significant amount of Lewis acid sites. Desilication process considered as selective extraction of silicon from zeolite framework assured increased concentration of acid sites. Indeed, the alkaline treated D-ZSM-5 revealed enhanced Brønsted and Lewis acidity in comparison with its bulk B-ZSM-5 counterpart. Bottom-up synthesized mesoporous zeolite M-ZSM-5 possessed slightly lowered amount of Brønsted acid sites and relatively high contribution of Lewis acid sites. As mentioned, the total concentration of acid sites detected with pyridine fully reproduced the aluminium concentration derived from chemical analysis, thus at our experimental conditions the diffusion of pyridine molecules was not limited even though the presence of high content of extra-framework species.

Information on the strength of acid sites was based on the comparison of (i) the values of the  $\Delta n_{\text{OH},\text{CO}}$  obtained in CO sorption and (ii) the results of pyridine thermodesorption experiments. The increasing strength of acidic Si(OH)Al groups is represented by more pronounced downshift of the Si(OH)Al group band perturbed by hydrogen bonding with CO molecule (the increasing  $\Delta\nu_{\text{OH},\text{CO}}$  value—Table 2). Among studied zeolites the highest  $\Delta\nu_{\text{OH},\text{CO}}$  values were found for microporous zeolites B-ZSM-5 and C-ZSM-5, thus the most acidic bridging hydroxyls are highly populated in those zeolites. Similar conclusion was withdrawn from Py thermodesorption experiments. The conservation of the  $1545\text{ cm}^{-1}$  ( $\text{PyH}^+$ ) and  $1455\text{ cm}^{-1}$  ( $\text{PyL}$ ) bands under the desorption temperature at  $350^\circ\text{C}$  was taken as a measure of the acid strength of the acid sites (Table 2). The lower strength of sites, the more disposed are Py molecules for desorption from acid sites. The reduced acid strength of Si(OH)Al groups was again observed for the micro/mesoporous zeolites. This observation is in line with literature data reporting that the external sites are less acidic than those in solely microporous channels.

### 3.2.3. Accessibility of protonic sites

Regarding the catalytic applications the material with model acidic properties i.e. the high concentration and strength of the acid sites as well as with the shape selective properties should also meet the proper accessibility of acid sites. The detailed characterization of accessibility of acid sites in studied zeolites was performed in fully quantitative manner using Pn (pivalonitrile) [28] as probe molecule. Even at room temperature the pivalonitrile molecules are able to reach through the 10-MR channels of zeolite the first available acid sites within the micropores mouths [28,29]. Consequently, the quantification of the acid sites exposed on mesopore surface and those hidden near to micropore mouths can be assessed. Furthermore, the sorption of Pn enables distinguishing among the accessibility of the Brønsted and Lewis acid sites. The values of the accessibility factors of pivalonitrile ( $\text{AF}_{\text{Pn}}$ ) for Brønsted and Lewis acid sites were calculated as the ratio of the concentrations of acid sites accessible to Pn molecules to those determined from sorption of pyridine (Table 2).

For all the studied materials the accessibility factor values were significantly higher for micro/mesoporous zeolites than for purely microporous ones. Even though the C-ZSM-5 sample is composed from small and highly agglomerated grains no substantial accessibility of acid sites was evidenced. The highest accessibility of protonic sites ( $\text{AF}_{\text{Pn}} = 60\%$ ) was observed for mesoporous M-ZSM-5 zeolite. Lower  $\text{AF}_{\text{Pn}}^{\text{B}}$  factors of both Brønsted and Lewis acid sites were recognized for desilicated zeolite. Additionally, enhanced accessibility of Lewis acid sites in hierarchical zeolites points to their high dispersion on mesopore surface.

### 3.3. Analysis of IR spectra of xylenes interacting with microporous and hierarchical zeolites

#### 3.3.1. Interaction of meta-xylene, ortho-xylene and para-xylene with zeolite

The basic requirement in quantitative IR studies is the determination of the molar extinction coefficient of the diagnostic band of probe molecule interacting with the specific adsorption site. Thus, there is need for an elaboration of experimental conditions in which the probe molecule reacts selectively with acid site according to known stoichiometry. The simplest and the most desired situation is when an each introduced probe molecule, for example one of the xylene isomer, reacts selectively with the one kind of the acid site solely, for example the Brønsted acid site. The sorption of the xylenes molecule seems to obey this condition. The IR spectra in the region of cycle vibrations of the xylenes and by-products of isomer-

**Table 2**

Concentration ( $\mu\text{mol g}^{-1}$ ) of the Al determined by chemical analysis ( $\text{Al}_{\text{ICP}}$ ), of the Brønsted (B) and Lewis (L) acid sites measured in quantitative experiments of pyridine (Py), pivalonitrile (Pn) together with respective accessibility factor ( $\text{AF}_{\text{Pn}}$ ). Acid strength of Brønsted sites measured as the downshift of the  $\text{Si(OH)Al}$  band perturbed by hydrogen bonding with CO molecule,  $\Delta\nu_{\text{OH,CO}}$ , as well as the strength of Brønsted and Lewis sites derived from Py-thermodesorption experiments.

Material	Si/Al	Concentration [ $\mu\text{mol g}^{-1}$ ]						Acid strength of sites				
		$\text{Al}_{\text{ICP}}$	Py	B	L	B + L	Pn	B	L	$\Delta\nu_{\text{OHCO}}$	Py	B
B-ZSM-5	32	471	390	34	424	48	7	0.12	0.21	315	0.95	1.00
C-ZSM-5	30	502	390	100	491	38	18	0.10	0.18	314	1.00	1.00
D-ZSM-5	22	680	582	100	682	233	63	0.40	0.63	309	0.90	1.00
M-ZSM-5	29	518	342	107	449	206	60	0.60	0.56	312	0.90	1.00

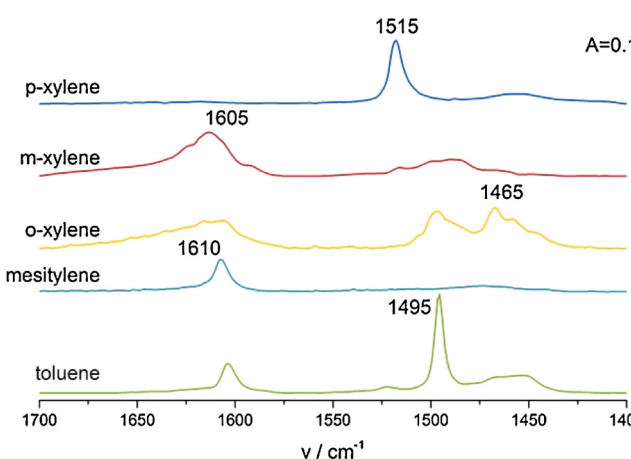


**Fig. 5.** IR spectra in region of cycle vibrations of the xylenes and by-products of isomerization (toluene and mesitylene) adsorbed on the B-ZSM-5 zeolite in room temperature.

ization (toluene and mesitylene) adsorbed on the B-ZSM-5 zeolite in room temperature are shown in Fig. 5.

To identify the diagnostic bands of xylenes interacting with Brønsted acid sites the sorption of each isomer was carried out on zeolite B-ZSM-5 possessing only negligible amount of Lewis acid sites. The interaction of the xylenes with Brønsted acid sites in B-ZSM-5 zeolite at room temperature resulted in the decrease of the  $\text{Si(OH)Al}$  band ( $3615\text{ cm}^{-1}$ ) and the appearance of the  $1605\text{ cm}^{-1}$ ,  $1515\text{ cm}^{-1}$  and  $1465\text{ cm}^{-1}$  bands attributed respectively to the *meta*-xylene, *para*-xylene and *ortho*-xylene bonded to Brønsted sites (Fig. 5). The selection of diagnostic bands was based on the results presented in paper of Thibault-Starzyk et al. [6], where the most intense negative covariance for these bands has been reported. The conditions required for quantitative measurement were ensured by both sorption of relatively small amounts of xylene isomers and a specified 10 min time delay before collecting the spectra enabling the diffusion of xylenes through 10 MR channel system of B-ZSM-5 zeolite. The second aspect worth underlining is the fact that the sorption of more bulky *ortho*- and *meta*-xylene isomers led to the interaction of probes not only with acidic  $\text{Si(OH)Al}$  groups but also with free  $\text{Si(OH)}$  groups. However, this interaction was negligible if enough small portion of probe molecule was introduced to IR cell. Consequently, the rule of the selective reaction of xylenes with Brønsted acid sites was fulfilled. The values of the absorption coefficients attained from the heights of the  $1605\text{ cm}^{-1}$ ,  $1515\text{ cm}^{-1}$  and  $1465\text{ cm}^{-1}$  bands attributed to the *meta*-xylene, *para*-xylene and *ortho*-xylene bonded to Brønsted acid sites were found to be equal of  $0.029 \pm 0.001\text{ cm}^2/\mu\text{mol}$ ,  $0.224 \pm 0.004\text{ cm}^2/\mu\text{mol}$  and  $0.024 \pm 0.001\text{ cm}^2/\mu\text{mol}$ , respectively. The absorption coefficient values obtained for *meta* and *ortho*-xylene are in good agreement with results presented in paper of Thibault-Starzyk et al.

[6], confirming the correctness of performed quantitative procedure. To the best of our knowledge the absorption coefficient of  $1515\text{ cm}^{-1}$  band representing the interaction of *para*-xylene with Brønsted acid sites has not been previously reported. The calculated absorption coefficients will be further used for quantitative evaluation of the products of catalytic reaction performed in IR quartz cell. The xylene isomerization process can also lead to formation of by-products, thus the absorption coefficients of  $1610\text{ cm}^{-1}$  and  $1495\text{ cm}^{-1}$  bands representative respectively for mesitylene and toluene interaction with Brønsted acid site were derived. The attained values of the absorption coefficients based on the heights of the  $1610\text{ cm}^{-1}$  and  $1495\text{ cm}^{-1}$  bands attributed to the mesitylene and toluene bonded to Brønsted acid sites were found to be equal of  $0.093 \pm 0.002\text{ cm}^2/\mu\text{mol}$  and  $0.172 \pm 0.001\text{ cm}^2/\mu\text{mol}$ .

### 3.3.2. 2D-COS analysis of isomerization of *o*-xylene over studied zeolites at 250 °C

The *ortho*-xylene isomerization over zeolites in the function of time can be considered as the external perturbation suitable for 2D COS analysis. For purposes of this study the series of spectra were collected during 15 min reaction time. Fig. 6 presents the results of synchronous correlation of series of spectra in the region of cycle vibrations of products of isomerization ( $1650\text{--}1360\text{ cm}^{-1}$ ) over purely microporous B-ZSM-5 and C-ZSM-5 zeolites. The analysis for hierarchical D-ZSM-5 and M-ZSM-5 is shown in Fig. 7. For clarity, the resulting 2D maps for each sample were divided into two separate graphs with positive and negative correlation peaks. Additionally, the 3D representations of correlation levels for all studied zeolites were included in Supporting information. The positive correlation between two separate bands represents the simultaneous increase or decrease in intensity of these bands. On the other hand, the negative correlation occurs when one of the bands changes its intensity at the expense of the other one. Thus, during *ortho*-xylene isomerization process following features should be observed: (i) the positive auto- and cross-peaks of bands of each isomer present in reaction (ii) the negative cross-peaks representing the transformation of bands of *o*-xylene to *m*-xylene or *p*-xylene.

The 2D COS analysis of the spectra recorded during the *o*-xylene isomerization at 250 °C allowed concluding that positive correlation (auto- and/or cross-peaks) for all studied samples, both microporous and hierarchical ones, can be observed for the bands representative for *m*-xylene ( $1623$ ,  $1605$ ,  $1592$ ,  $1484$  and  $1382\text{ cm}^{-1}$ ), *o*-xylene ( $1497$ ,  $1465$ ,  $1428$  and  $1414\text{ cm}^{-1}$ ) and *p*-xylene ( $1515\text{ cm}^{-1}$ ). For all studied samples the positive correlation was also found between bands of *p*-xylene ( $1515\text{ cm}^{-1}$ ) and *m*-xylene ( $1623$ ,  $1605$ ,  $1592\text{ cm}^{-1}$ ) pointing to coincident formation of both isomers. Only for microporous B-ZSM-5 and C-ZSM-5 the positive correlation was also found for additional bands of *p*- and *m*-xylene ( $1515\text{ cm}^{-1} \sim 1484\text{ cm}^{-1}$ ). What is more, in the case of hierarchical D-ZSM-5 and M-ZSM-5 zeolites the positive correlation between the bands of both *p*-xylene and *m*-xylene ( $1515$  and  $1623\text{ cm}^{-1}$ ) and the band of mesitylene ( $1610\text{ cm}^{-1}$ ) confirmed the formation of mesitylene as by-product formed by xylenes dispro-

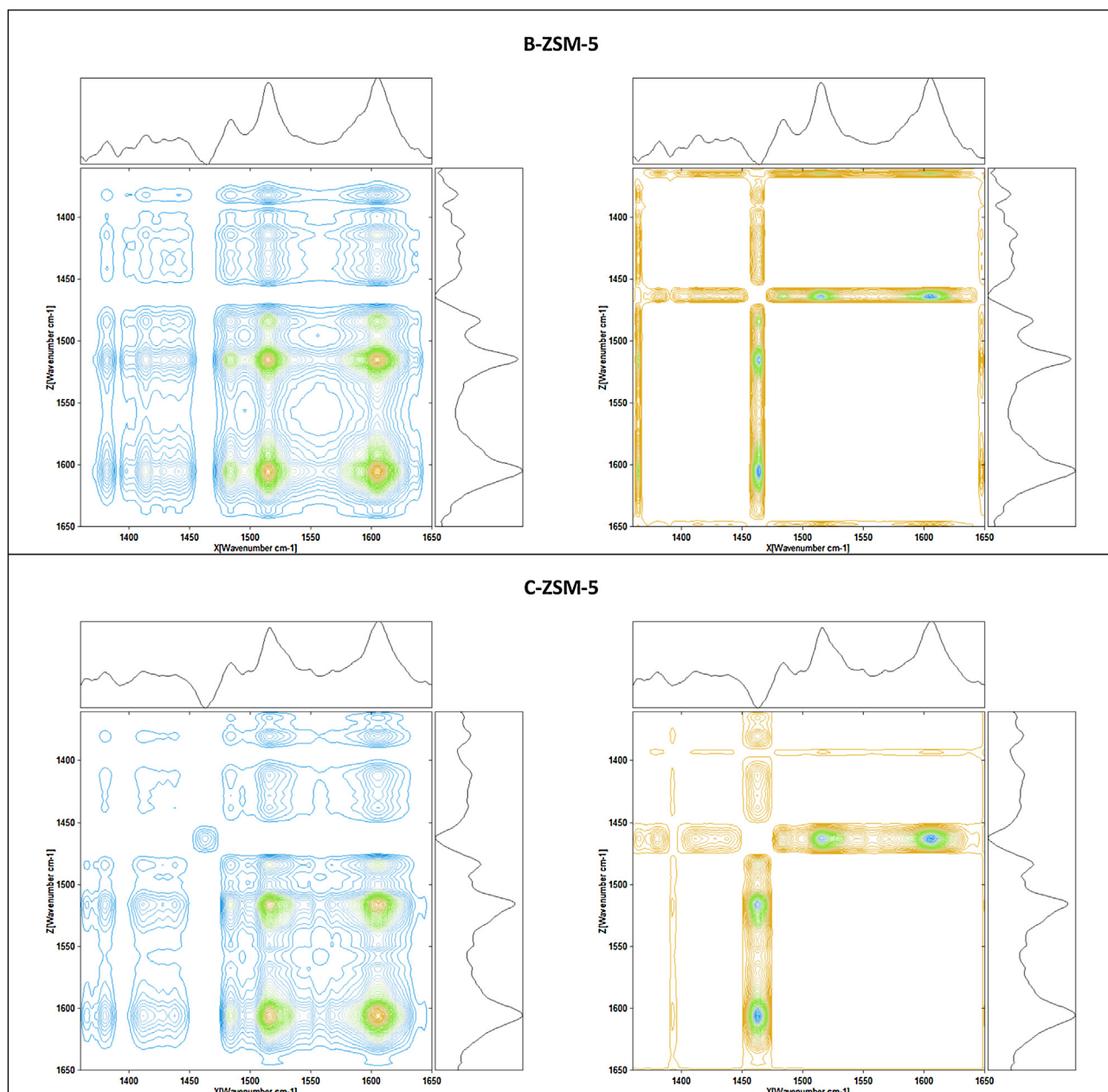


**Fig. 6.** Positive (right) and negative (left) part of the 2D synchronous correlation map of *ortho*-xylene isomerization reaction at 250 °C for microporous zeolites B-ZSM-5 and C-ZSM-5. Top and right projection represent the change of correlation level at 1515 cm<sup>-1</sup>.

portionation. Xylenes disproportionation leads to the production of toluene as the second product. However, the diagnostic bands of toluene (1604 and 1495 cm<sup>-1</sup>) overlap with the bands of *m*-xylene and *o*-xylene thus the toluene production is difficult to be detected in IR spectra. However the formation of toluene can be tentatively confirmed by negative correlation between the 1495 cm<sup>-1</sup> band of toluene and 1623 and 1515 cm<sup>-1</sup> bands of *m*-xylene and *p*-xylene, respectively. Still however, the negative correlation between the *o*-xylene (1465 cm<sup>-1</sup>) and mesitylene (1610 cm<sup>-1</sup>) bands observed only for hierarchical zeolites confirms that mesoporous zeolites as catalysts in isomerization of xylene are less selective and the formation of bulky by-products as mesitylene (or others in no detectable amounts) is also effective. Consequently, the formation of toluene was derived from the presence of mesitylene and above mentioned negative correlation between the 1495 cm<sup>-1</sup> band of toluene and the bands of *m*-xylene (1623 cm<sup>-1</sup>) and *p*-xylene (1515 cm<sup>-1</sup>).

For all studied zeolites the negative correlation was also found between the bands of *o*-xylene (1465 cm<sup>-1</sup>) and bands of both *p*-xylene and *m*-xylene (1605 and 1515 cm<sup>-1</sup>, resp.). It can be noticed that the C-ZSM-5 sample with highly agglomerated small grains demonstrated more pronounced than B-ZSM-5 sample correlation level between the above mentioned bands, what is well presented on 3D representations of correlation levels (Supporting information). The textural properties of C-ZSM-5 sample seem to facilitate the occurrence of isomerization process. These conclusions are supported by the results of quantitative evaluation of reaction products presented in Section 3.3.3. Less selective character of hierarchical zeolites in the case of xylene isomerization reaction has been also presented in work of Fernandez et al. [23], where authors widely discussed the formation and nature of coke species formed during reaction.

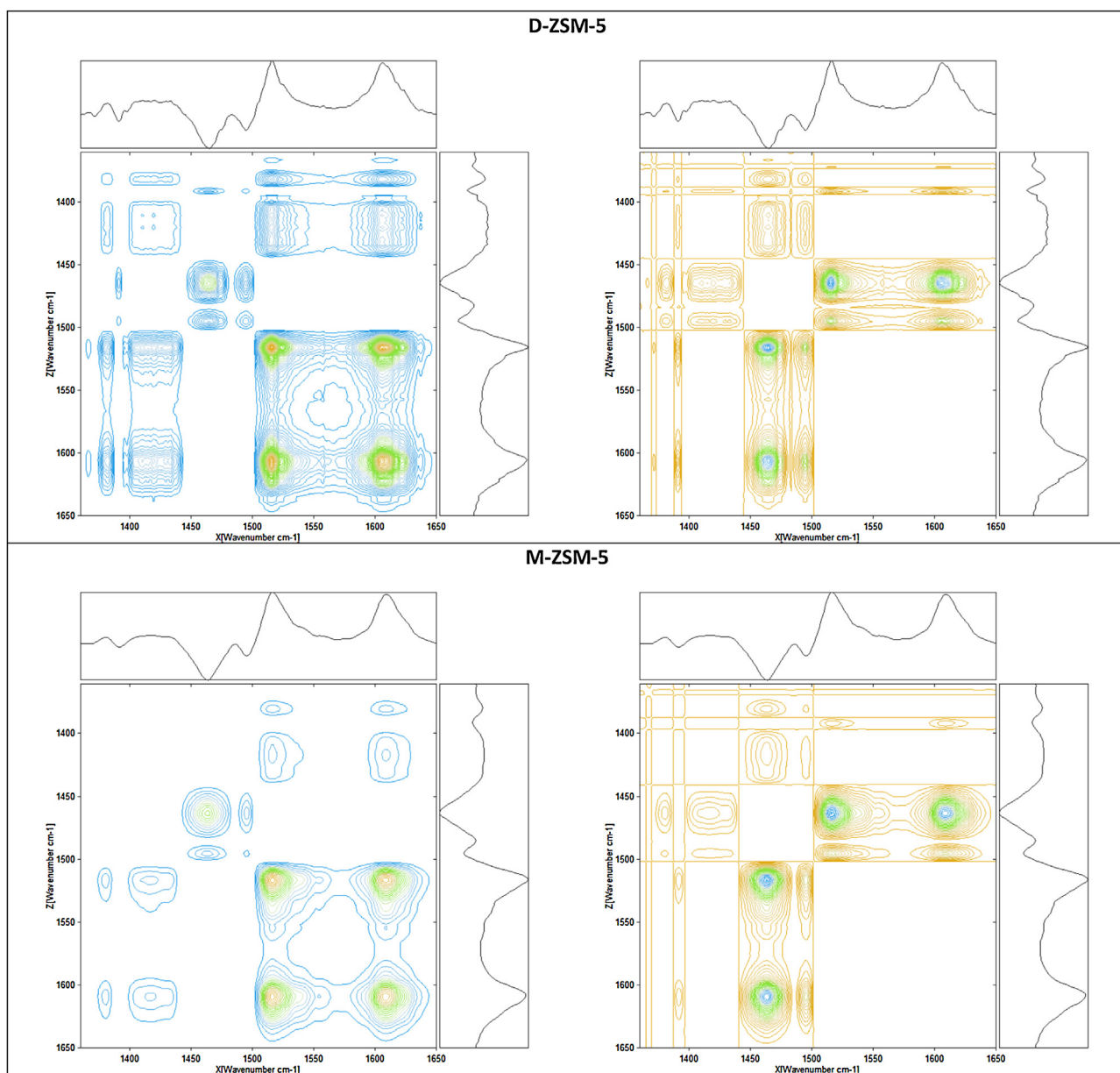


**Fig. 7.** Positive (right) and negative (left) part of the 2D synchronous correlation map of *ortho*-xylene isomerization reaction at 250 °C for hierarchical zeolites D-ZSM-5 and M-ZSM-5. Top and right projection represent the change of correlation level at 1515 cm<sup>-1</sup>.

### 3.3.3. 2D-COS analysis of isomerization of *m*-xylene over studied zeolites at 250 °C

Similarly as presented above the *meta*-xylene isomerization was carried out for 15 min in quartz IR cell and the collected spectra were analysed with the use of 2D COS method. The resulting 2D maps of synchronous correlation in the region of cycle vibrations of products of isomerization (1650–1360 cm<sup>-1</sup>) were divided into the positive and negative parts and they are presented in Fig. 8 for microporous zeolites and in Fig. 9 for hierarchical ones. Additionally, the 3D representations of correlation levels for all studied zeolites were included in Supporting information. In the case of *m*-xylene isomerization process the following features should be observed: (i) the positive auto- and cross-peaks of bands of each isomer present in reaction (ii) the negative cross-peaks representing the transformation of bands of *m*-xylene to *o*-xylene or *p*-xylene. The *m*-xylene isomer being the bulkiest of all xylene isomers retains in zeolite structure and its diffusion through 10 MR channels is limited.

The 2D COS analysis of the spectra recorded in 15 min reaction time of the *m*-xylene isomerization at 250 °C over microporous and hierarchical zeolites clearly revealed their porous characteristic. The positive correlations seen as auto- and/or cross-peaks independently from the type of zeolite were found for the bands of *m*-xylene (1623, 1605, 1484 and 1382 cm<sup>-1</sup>), *o*-xylene (1497 and 1465 cm<sup>-1</sup>) and *p*-xylene (1515 cm<sup>-1</sup>). However, the overall correlation level for auto-peaks differed among samples depending on porosity type. Desilication process did not influence the character of *m*-xylene interaction with zeolite surface i.e. the obtained 2D COS maps of purely microporous B-ZSM-5 and hierarchical D-ZSM-5 are quite similar, a strongly different behaviour was observed for hierarchical M-ZSM-5 zeolite. This zeolite possesses enhanced mesopore surface area S<sub>meso</sub> resulting from small (diameter of around 10 nm) and regularly distributed mesopores within zeolite grains (Table 1, Fig. 2) and the highest amount of silanols groups on surface grains (Fig. 4). These textural and spectroscopic properties did not significantly affect the *o*-xylene isomerization described above and

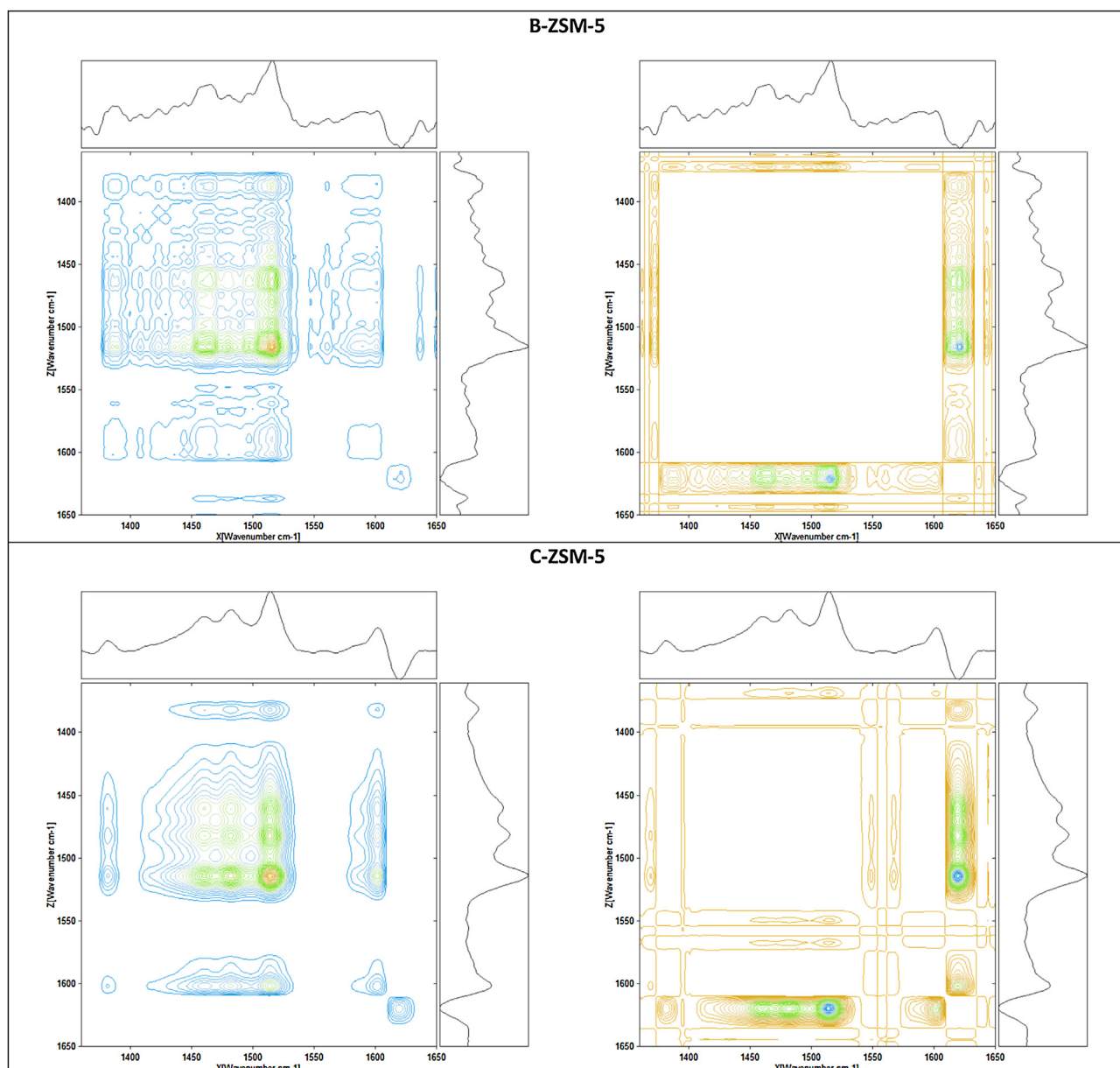


**Fig. 8.** Positive (right) and negative (left) part of the 2D synchronous correlation map of *meta*-xylene isomerization reaction at 250 °C for microporous zeolites B-ZSM-5 and C-ZSM-5. Top and right projection represent the change of correlation level at 1515 cm<sup>-1</sup>.

similar results were found for M-ZSM-5 and D-ZSM-5 samples. However, in the case of more bulky *m*-xylene molecule the different type of porosity in M-ZSM-5 sample seems to have an impact on the isomerization process. As it can be seen from 2D correlation maps the newly arising band at 1634 cm<sup>-1</sup> negatively correlates with the 1605 and 1484 cm<sup>-1</sup> bands of *m*-xylene as well as the 1497 cm<sup>-1</sup> band of *o*-xylene. Thus, we assume that the band of 1634 cm<sup>-1</sup> is representative for coke precursors. The textural properties of M-ZSM-5 i.e. large mesopore surface area with high amount of silanol groups prompted the formation of coke precursors. The differences between the M-ZSM-5 sample and the other ones were noticed also in positive part of 2D correlation maps. The highest correlation level of auto-peaks for B-ZSM, C-ZSM-5 and D-ZSM-5 is observed for *p*-xylene band at 1515 cm<sup>-1</sup>. On the other hand, for M-ZSM-5 sample the highest correlation level in auto-peaks is seen for 1605 cm<sup>-1</sup> band of *m*-xylene. Thus, it can be concluded that in the case of former zeolites the increase of intensity of *p*-xylene band is the most dominating variation in the spectrum during the *m*-xylene

isomerization, what is also well presented on 3D representations of correlation levels (Supporting information). For M-ZSM-5 sample the most significant alteration was observed for 1605 cm<sup>-1</sup> of *m*-xylene band, which intensity gradually dropped during the reaction time. Thus it can be concluded that the highest amount of *m*-xylene was sorbed on the surface of M-ZSM-5 zeolite, what is justified in the high surface area with large amount of silanol groups as sorption sites for xylene.

The 2D correlation related to the formation of *p*-xylene and *o*-xylene was also found for B-ZSM-5, C-ZSM-5 and D-ZSM-5 samples. The positive correlation between the bands of *p*-xylene (1515 cm<sup>-1</sup>) and *o*-xylene (1497 and 1465 cm<sup>-1</sup>) indicates a simultaneous formation of both isomers. However, the positive correlation was also found between the bands of *m*-xylene (1484, 1605 cm<sup>-1</sup>) and both of *p*-xylene (1515 cm<sup>-1</sup>) and *o*-xylene (1465 cm<sup>-1</sup>), what demonstrates that in our experimental conditions not only isomerization process but also the on-going sorption of *m*-xylene take place. This phenomenon was not observed for *o*-

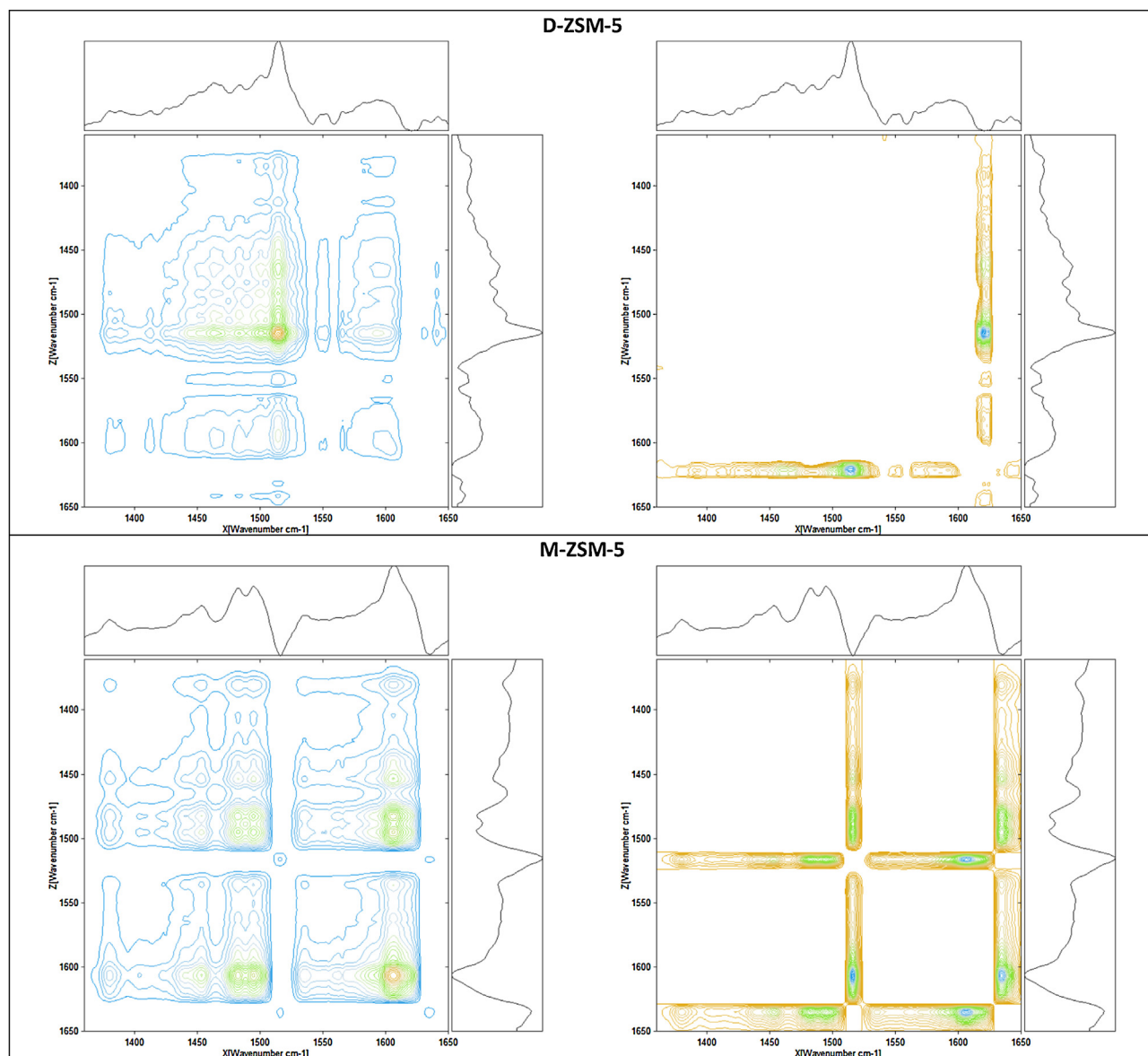


**Fig. 9.** Positive (right) and negative (left) part of the 2D synchronous correlation map of neta-xylene isomerization reaction at 250 °C for hierarchical zeolites D-ZSM-5 and M-ZSM-5. Top and right projection represent the change of correlation level at 1515 cm<sup>-1</sup>.

xylene isomerization process. Thus it can be anticipated that the diffusion of *m*-xylene molecules is largely restricted by size limitations and even at temperatures as high as 250 °C the transport to active sites through 10 MR channel of zeolite is limited and requires longer period of time.

Diverse observations on the basis of 2D COS maps were done for M-ZSM-5 sample, where the positive correlation between the bands of *m*-xylene (1605 cm<sup>-1</sup>) and *o*-xylene (1497 and 1484 cm<sup>-1</sup>) points to simultaneous transformation of these molecules either to *p*-xylene or to mentioned earlier coke precursors. As can be expected the negative correlation between the band of *p*-xylene (1515 cm<sup>-1</sup>) and the bands of both *m*-xylene (1605 cm<sup>-1</sup>) and *o*-xylene was also found (1497 and 1484 cm<sup>-1</sup>). This negative correlation was only evidenced for M-ZSM-5 sample. Contrary to other samples, on the surface of M-ZSM-5 sample isomerization process occurs without on-going sorption of *m*-xylene. This result can be related with highly porous character of M-ZSM-5 with enhanced accessibility of sites being the centres of xylene sorption.

### 3.3.4. Quantitative evaluation of xylene isomerization process over studied zeolites

In situ IR spectroscopy quantitative studies of *ortho*- and *meta*-xylene isomerization processes were performed in order to determine the influence of acidity and porosity of zeolites on their catalytic performance. Despite obvious limitations of in situ IR studies, the presented results provide noteworthy insight in xylene isomerization reaction over hierarchical zeolites. The xylene isomerization process was performed in quartz IR cell at 250 °C for 15 min, after this period of time the quartz cell was cooled down to room temperature and then the IR spectra of reaction products were gathered. Conversion, selectivity and yield were calculated on the basis of IR quantitative measurements of reaction products with employ of the presented earlier extinction coefficients.

The 2D COS analysis results (Sections 3.3.1 and 3.3.2.) proved that isomerization of *o*-xylene over hierarchical zeolites led to the formation of by-products. The formation of by-products was even detected at 1D IR spectra after isomerization process (Fig. 10). It is clearly seen that for hierarchical zeolite the mesitylene (band at

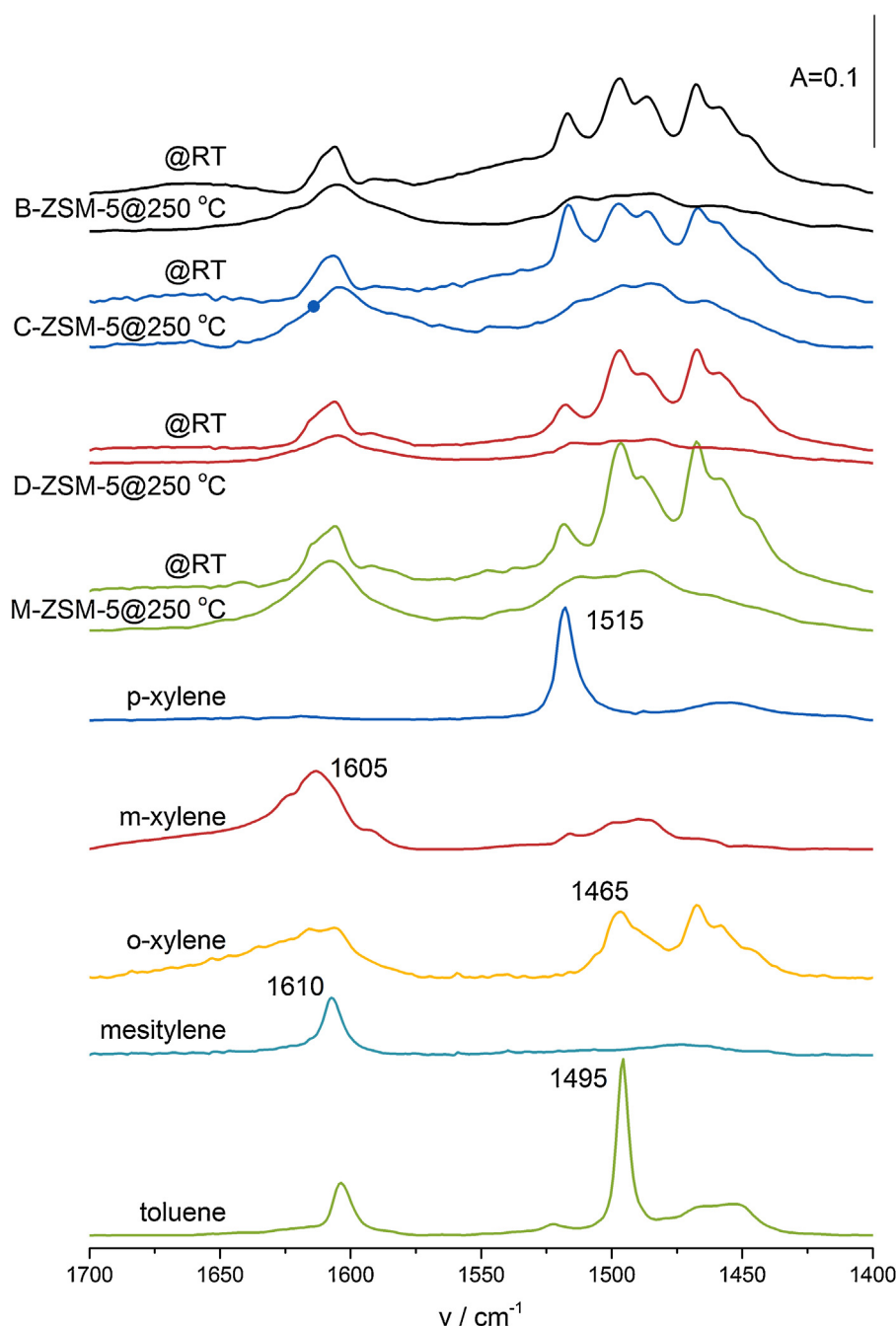


**Fig. 10.** IR spectra in region of cycle vibrations of the xylenes and by-products of isomerization (toluene and mesitylene) after *o*-xylene isomerization at 250 °C for all studied zeolites.

1610 cm<sup>-1</sup>) is easily produced. The quantitative IR studies (Table 3) revealed that the zeolites offered moderate and comparable activity in xylene isomerization, however in this study the main attention will be paid on the differences in selectivity to desired products. It can be noticed that for purely microporous B-ZSM-5 and C-ZSM-5 zeolites higher selectivity to the most desired product i.e. *p*-xylene, was achieved. This result can be directly related to high abundance of microporous environment giving rise to shape selectivity. The another important factors influencing the activity of C-ZSM-5 sample are the textural properties. It seems that the spherical shape of small aggregated grains with limited mesopore surface area assured higher conversion and higher selectivity to desired *p*-xylene product. Considering the results of 2D COS analysis pointing to (i) coincident formation of both *p*-xylene and *m*-xylene iso-

mers and (ii) the transformation of the *o*-xylene to both *p*-xylene and *m*-xylene (negative correlation between the bands of *o*-xylene (1465 cm<sup>-1</sup>) and bands of both *p*-xylene and *m*-xylene (1605 and 1515 cm<sup>-1</sup>, resp.)) it can be concluded that at given experimental conditions the monomolecular mechanism with direct conversion between the *o*-xylene and *p*-xylene occurred in 10 MR pores. Similar results of the conversion between the *o*-xylene and *p*-xylene was observed by Goncalves et al. [30] and Young et al. [31], when temperature of reaction above 200 °C has been applied. On the other hand, the mesoporosity fabricated by desilication and gemini-surfactant assisted rout did not significantly affect the catalytic performance but at the same time led to decrease of *p*-xylene selectivity. It is worth underlining that acid sites easily available from external surface can privilege bimolecular reactions leading

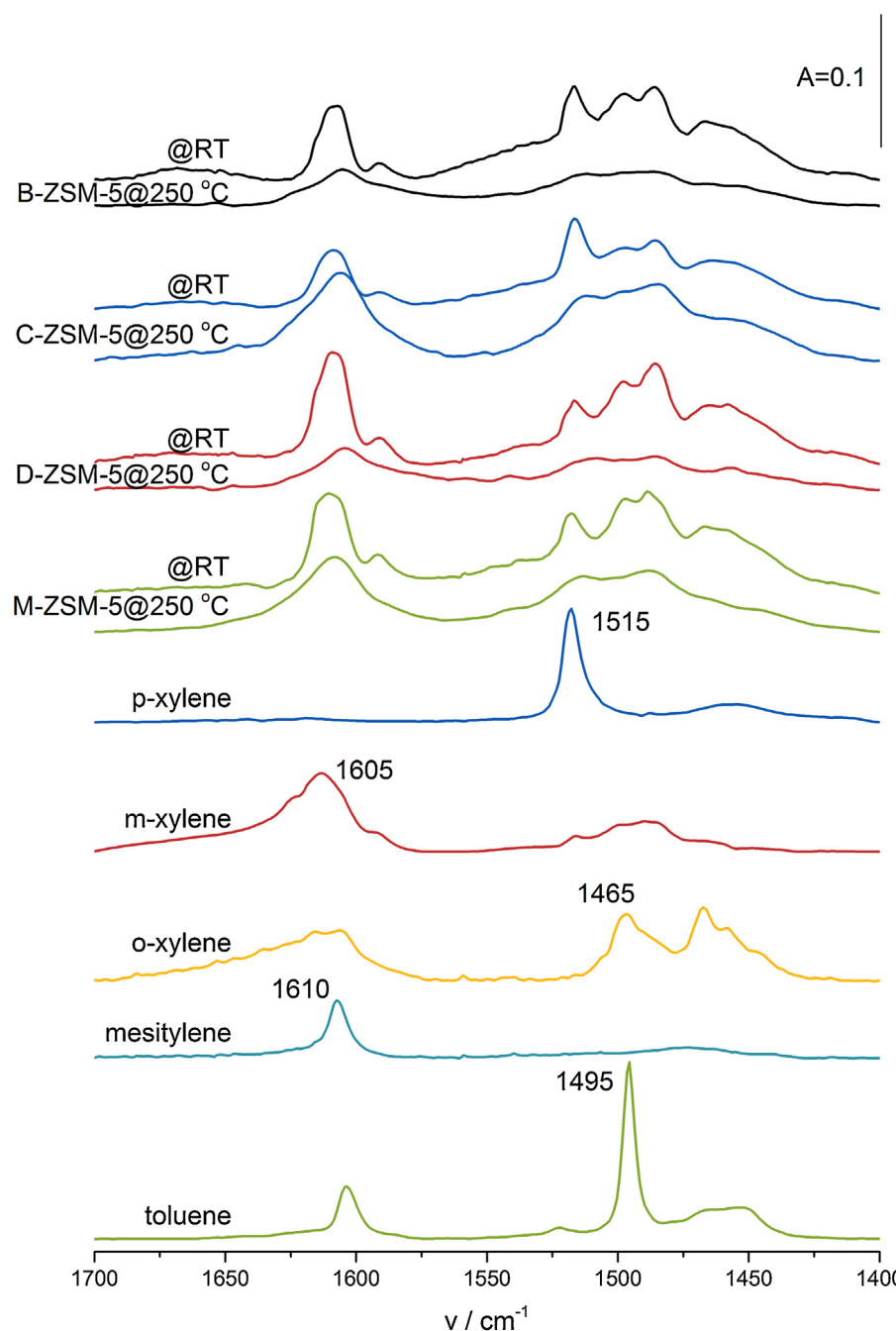


**Fig. 11.** IR spectra in region of cycle vibrations of the xylenes and by-products of isomerization (toluene and mesitylene) after *m*-xylene isomerization at 250 °C for all studied zeolites.

to by-products or catalyst coking [32,33]. The highest contribution of by-products was found for M-ZSM-5 zeolite, what is in agreement with the most mesoporous character of this sample, thus the highest accessibility of acid sites.

In the case of *m*-xylene isomerization only the presence of xylene isomers was confirmed, the products originating from disproportionation reaction were detected neither in 2D COS analysis nor in 1D IR spectrum after reaction (Table 4, Fig. 11). The highest activity was found for C-ZSM-5 with almost twice higher conversion in comparison with mesoporous zeolites D-ZSM-5 and M-ZSM-5. Similar trend was observed when considering the selectivity to *p*-xylene i.e. the most desired product. The highest values of *p*-xylene selectivity were observed for microporous B-ZSM-5 and C-ZSM-5 zeolites. It seems that in the case of *m*-xylene iso-

merization better activity of C-ZSM-5 zeolite is a result of not only the specific textural properties but also the optimal acidity. Higher values of conversion should be related to the increase of the concentration and the strength of acid sites. Thus, it can be concluded that the moderate amount of Brønsted acid sites in C-ZSM-5 sample together with considerably high amount of Lewis acid sites are optimal for enhanced conversion. Significantly higher concentration of acid sites (as for D-ZSM-5) or enhanced mesopore surface area (as for D-ZSM-5 and M-ZSM-5) led to decrease in selectivity and conversion of isomerization process. The work of Cejka and Wichterlova [3] showed that zeolites with lower acidity can provide higher activity under specific reaction condition. Furthermore, in paper of Perez-Pariente et al. [34] it has been proved that maximum activity of studied zeolite Beta was observed for zeo-

**Table 3**

Catalytic performance of studied zeolites in o-xylene isomerization process performed in quartz IR cell at 250 °C for 15 min. The results obtained from IR spectra recorded after reaction at RT.

Material	Product	Yield [%]	Selectivity [%]	Conversion [%]
B-ZSM-5	m-xylene	30%	87%	35%
	p-xylene	4%	13%	
	o-xylene	65%		
C-ZSM-5	m-xylene	33%	83%	40%
	p-xylene	7%	17%	
	o-xylene	60%		
D-ZSM-5	m-xylene	25%	74%	35%
	p-xylene	3%	8%	
	o-xylene	65%		
	mesitylene	3%	10%	
	Toluene	3%	9%	
M-ZSM-5	m-xylene	27%	67%	40%
	p-xylene	4%	9%	
	o-xylene	60%		
	mesitylene	5%	11%	
	Toluene	5%	13%	

**Table 4**

Catalytic performance of studied zeolites in m-xylene isomerization process performed in quartz IR cell at 250 °C for 15 min. The results obtained from IR spectra recorded after reaction at RT.

Material	Product	Yield [%]	Selectivity [%]	Conversion [%]
B-ZSM-5	m-xylene	72%		28%
	p-xylene	8%	29%	
	o-xylene	20%	71%	
C-ZSM-5	m-xylene	62%		38%
	p-xylene	10%	28%	
	o-xylene	27%	72%	
D-ZSM-5	m-xylene	78%		22%
	p-xylene	4%	19%	
	o-xylene	18%	81%	
M-ZSM-5	m-xylene	76%		24%
	p-xylene	6%	23%	
	o-xylene	19%	77%	

lites with Si/Al ratios between 14 and 15, what corresponded to the optimum amount of Brønsted and Lewis acid sites. The differences in catalytic performance between the C-ZSM-5 and B-ZSM-5 sample can be associated both with the lower amount of Lewis acid sites enhancing Brønsted acidity and textural properties especially the shape of zeolite grains. The presence of mesopores in studied samples strongly influenced their catalytic performance favouring non-selective reactions and the most probably leading to coking. The isomerization of m-xylene, as the most bulky among all xylene isomers, performed over hierarchical zeolites with high accessibility of acid sites seems to be strongly affected by thermodynamics of xylene isomerization process [35]. Low conversion of m-xylene over hierarchical zeolites confirmed its high stability in non-shape selective environment.

#### 4. Conclusions

This work was attempted to offer an insight into xylene isomerization process in the terms of acidity and porosity picture of microporous and hierarchical zeolites ZSM-5. The isomerization reaction was followed by 2D COS analysis of IR spectra and gave insight into reaction mechanism. The selection of the studied materials, from microporous ZSM-5 to their hierarchical analogues obtained by different methods allowed following the influence of porosity and acidity on xylene sorption and isomerization processes. It was shown that the microporous character of zeolites

was crucial for high selectivity to the most desired product i.e. p-xylene. However, it was found that even for purely microporous zeolites the size and shape of zeolite grains were crucial for activity and selectivity during catalytic reaction. In the case of mesoporous zeolites the formation of mesitylene and toluene as by-products was confirmed. Furthermore, for hierarchical zeolites the high amount of silanols groups prompted coke formation on highly developed external surface. The isomerization of m-xylene, the bulkiest among xylene isomers, performed over hierarchical zeolites was affected by thermodynamics of xylene isomerization process rather than the presence of shape selective micropore environment.

#### Acknowledgement

The work was financed by Grant No. 2014/13/D/ST5/02761 from the National Science Centre, Poland.

#### Appendix A. Supplementary data

Supplementary data associated with this article can be found, in the online version, at <http://dx.doi.org/10.1016/j.cattod.2016.02.035>.

#### References

- [1] J. Weitkamp, Zeolites and catalysis, Solid State Ionics 131 (2000) 175–188.
- [2] J. Weitkamp, M. Hunger, Acid and base catalysis on zeolites, in: J. Čejka, H. van Bekkum, A. Corma, F. Schüth (Eds.), Studies in Surface Science and Catalysis, Elsevier, 2007, pp. 787–835.
- [3] J. Čejka, B. Wichterlová, Acid-catalyzed synthesis of mono- and dialkyl benzenes over zeolites: active sites, zeolite topology, and reaction mechanisms, Catal. Rev. Sci. Eng. 44 (2002) 375–421.
- [4] A. Corma, A. Cortes, I. Nebot, F. Tomas, On the mechanism of catalytic isomerization of xylenes. Molecular orbital studies, J. Catal. 57 (1979) 444–449.
- [5] I. Noda, Generalized two-dimensional correlation method applicable to infrared, Raman, and other types of spectroscopy, Appl. Spectrosc. 47 (1993) 1329–1336.
- [6] F. Thibault-Starzyk, A. Vimont, J.-P. Gilson, 2D-COS IR study of coking in xylene isomerisation on H-MFI zeolite, Catal. Today 70 (2001) 227–241.
- [7] Y. Liu, W. Zhang, T.J. Pinnavaia, Steam-stable MSU-S aluminosilicate mesostructures assembled from zeolite ZSM-5 and zeolite beta seeds, Angew. Chem. Int. Ed. 40 (2001) 1255–1258.
- [8] I. Schmidt, A. Boisen, E. Gustavsson, K. Ståhl, S. Pehrson, S. Dahl, A. Carlsson, C.J.H. Jacobsen, Carbon nanotube templated growth of mesoporous zeolite single crystals, Chem. Mater. 13 (2001) 4416–4418.
- [9] M. Choi, H.S. Cho, R. Srivastava, C. Venkatesan, D.-H. Choi, R. Ryoo, Amphiphilic organosilane-directed synthesis of crystalline zeolite with tunable mesoporosity, Nat. Mater. 5 (2006) 718–723.
- [10] H. Wang, T.J. Pinnavaia, MFI zeolite with small and uniform intracrystal mesopores, Angew. Chem. Int. Ed. 45 (2006) 7603–7606.
- [11] I.I. Ivanova, E.E. Knyazeva, Micro-mesoporous materials obtained by zeolite recrystallization: synthesis, characterization and catalytic applications, Chem. Soc. Rev. 42 (2013) 3671–3688.
- [12] S. Mintova, J.-P. Gilson, V. Valtchev, Advances in nanosized zeolites, Nanoscale 5 (2013) 6693–6703.
- [13] C.J. Van Oers, K. Gora-Marek, K. Sadowska, M. Mertens, V. Meynen, J. Datka, P. Cool, In situ IR spectroscopic study to reveal the impact of the synthesis conditions of zeolite beta nanoparticles on the acidic properties of the resulting zeolite, Chem. Eng. J. 237 (2014) 372–379.
- [14] K. Sadowska, K. Gora-Marek, M. Drodzak, P. Kustrowski, J. Datka, J. Martinez Triguero, F. Rey, Desilication of highly siliceous zeolite ZSM-5 with NaOH and NaOH/tetrabutylamine hydroxide, Microporous Mesoporous Mater. 168 (2013) 195–205.
- [15] D. Verboekend, M. Milina, S. Mitchell, J. Pérez-Ramírez, Hierarchical zeolites by desilication: occurrence and catalytic impact of recrystallization and restructuring, Cryst. Growth Des. 13 (2013) 5025–5035.
- [16] S. Abelló, A. Bonilla, J. Pérez-Ramírez, Mesoporous ZSM-5 zeolite catalysts prepared by desilication with organic hydroxides and comparison with NaOH leaching, Appl. Cata. A: Gen. 364 (2009) 191–198.
- [17] M. Müller, G. Harvey, R. Prins, Comparison of the dealumination of zeolites beta, mordenite ZSM-5 and ferrierite by thermal treatment, leaching with oxalic acid and treatment with SiCl4 by 1H, 29Si and 27Al MAS NMR, Microporous Mesoporous Mater. 34 (2000) 135–147.
- [18] R.A. Beyerlein, G.B. McVicker, L.N. Yacullo, J.J. Ziemiak, The influence of framework and nonframework aluminum on the acidity of high-silica,

- proton-exchanged FAU-framework zeolites, *J. Phys. Chem.* 92 (1988) 1967–1970.
- [19] D.C. Koningsberger, J.T. Miller, W.N.D.E.I.a.A.T.B. Joe, W. Hightower, *The Development of Strong Acidity by Non-framework Aluminum in H-USY Determined by Al XAFS Spectroscopy*, Studies in Surface Science and Catalysis, Elsevier, 1996, pp. 841–850.
- [20] D. Verboekend, J. Perez-Ramirez, Design of hierarchical zeolite catalysts by desilication, *Catal. Sci. Technol.* 1 (2011) 879–890.
- [21] K. Sadowska, K. Gora-Marek, J. Datka, Hierarchic zeolites studied by IR spectroscopy: acid properties of zeolite ZSM-5 desilicated with NaOH and NaOH/tetrabutylamine hydroxide, *Vib. Spectrosc.* 63 (2012) 418–425.
- [22] F. Thibault-Starzyk, A. Vimont, C. Fernandez, J.-P. Gilson, 2D correlation IR spectroscopy of xylene isomerisation on H-MFI zeolite, *Chem. Commun.* (2000) 1003–1004.
- [23] C. Fernandez, I. Stan, J.-P. Gilson, K. Thomas, A. Vicente, A. Bonilla, J. Pérez-Ramírez, Hierarchical ZSM-5 zeolites in shape-selective xylene isomerization: role of mesoporosity and acid site speciation, *Chem. A Eur. J.* 16 (2010) 6224–6233.
- [24] J. Rouquerol, P. Llewellyn, F. Rouquerol, F.R.-R.J.R.a.N.S.P.L. Llewellyn, Is the BET equation applicable to microporous adsorbents? *Stud. Surf. Sci. Catal.* (2007) 49–56 (Elsevier).
- [25] E.P. Barrett, L.G. Joyner, P.P. Halenda, The determination of pore volume and area distributions in porous substances. I. Computations from nitrogen isotherms, *J. Am. Chem. Soc.* 73 (1951) 373–380.
- [26] K. Góra-Marek, M. Derewiński, P. Sarv, J. Datka, IR and NMR studies of mesoporous alumina and related aluminosilicates, *Catal. Today* 101 (2005) 131–138.
- [27] K. Góra-Marek, K. Tarach, M. Choi, 2,6-Di-*tert*-butylpyridine sorption approach to quantify the external acidity in hierarchical zeolites, *J. Phys. Chem. C* 118 (2014) 12266–12274.
- [28] K. Sadowska, K. Gora-Marek, J. Datka, Accessibility of acid sites in hierarchical zeolites: quantitative IR studies of pivalonitrile adsorption, *J. Phys. Chem. C* 117 (2013) 9237–9244.
- [29] K. Mlekodaj, K. Tarach, J. Datka, K. Gora-Marek, W. Makowski, Porosity and accessibility of acid sites in desilicated ZSM-5 zeolites studied using adsorption of probe molecules, *Microporous Mesoporous Mater.* 183 (2014) 54–61.
- [30] J.C. Gonçalves, A.E. Rodrigues, Xylene isomerization in the liquid phase using large-pore zeolites, *Chem. Eng. Technol.* (2016) (n/a-n/a).
- [31] L.B. Young, S.A. Butter, W.W. Kaeding, Shape selective reactions with zeolite catalysts: III. Selectivity in xylene isomerization, toluene-methanol alkylation, and toluene disproportionation over ZSM-5 zeolite catalysts, *J. Catal.* 76 (1982) 418–432.
- [32] M. Paciga, A. Smiešková, P. Hudec, Z. Židek, Contribution of particle size and aluminium distribution to the para-selectivity of ZSM-5 type zeolites, *React. Kinet. Catal. Lett.* 60 (1997) 21–26.
- [33] D. Fraenkel, Role of external surface sites in shape-selective catalysis over zeolites, *Ind. Eng. Chem. Res.* 29 (1990) 1814–1821.
- [34] J. Pérez-Pariente, E. Sastre, V. Fornés, J.A. Martens, P.A. Jacobs, A. Corma, Isomerization and disproportionation of *m*-xylene over zeolite  $\beta$ , *Appl. Catal.* 69 (1991) 125–137.
- [35] J.C. Gonçalves, A.E. Rodrigues, Thermodynamic equilibrium of xylene isomerization in the liquid phase, *J. Chem. Eng. Data* 58 (2013) 1425–1428.